Research Article ISSN 2639-9458

Microbiology & Infectious Diseases

NutraNanoSpheres for Nutraceutical Delivery Systems in Human Diseases

Jerry T Thornthwaite[1,*], Daniel Strasser[1,2] and Olufemi Akanni[1,3]

[1]*Cancer Research Institute of West Tennessee Henderson, Tennessee, USA.*

[2]*miVital, St. Galen, CH.*

[3]*Osun State University Osun State, Nigeria.*

[*]Correspondence:
Jerry T Thornthwaite, Cancer Research Institute of West Tennessee Henderson, Tennessee, USA.

Received: 14 Jun 2025; **Accepted:** 17 Jul 2025; **Published:** 27 Jul 2025

Citation: Jerry T Thornthwaite, Daniel Strasser, Olufemi Akanni. NutraNanoSpheres for Nutraceutical Delivery Systems in Human Diseases. Microbiol Infec Dis. 2025; 9(4): 1-17.

ABSTRACT

To demonstrate the significance of NutraNanoSphere (NNS) technology, we have selected three medical applications that highlight the profound impact of our medical research on cognitive development, malaria prevention, and cancer treatment. As examples, we show three applications: one using a single molecule, Choline, that affects cognitive brain development by allowing it to cross the blood-brain barrier, another using four NNS in the same preparation to cure malaria in babies, and final two examples to show the importance of the NNS for bioavailability and accessibility where NNS Vitamin C or NNS Curcumin enters the cancer stem cell intact show a dramatic ability to kill the cancer stem cells after their penetration. Our early discovery of what is now called the Natural Killer Cell (NKC) and the Cancer Stem Cells (CSCs) is presented. The importance of plant botanicals, specifically Curcumin and Vitamin C, will be demonstrated to highlight their role in targeting CSCs unaffected by current classical cancer treatment methods. Finally, a review of the essential neutraceuticals involved in killing CSCs is presented.

Keywords

Human Diseases, Cell Counting, Chemical modifications.

Introduction

A significant proportion of pharmaceutical drugs have poor water solubility. It is commonly cited in pharmaceutical sciences that approximately 40–90% of new chemical entities discovered through new drug discovery programs are poorly water-soluble, with about 90% of the drugs in the development pipeline are poorly water-soluble [1]. Poor water solubility can limit a drug's absorption in the body, reducing its bioavailability and therapeutic effectiveness. Developing formulations that improve solubility is a major challenge in pharmaceutical development.

Aging, neurological disorders (like stroke or Parkinson's), dry mouth, and certain medical conditions can make swallowing more difficult. Many elderly patients must take 20+ pills, resulting in appetite loss and wasting. The swallowing issues lead to patients skipping dosages, resulting in a reduction in the effectiveness of treatment. Therefore, difficulty swallowing pills is a significant issue, particularly for elderly patients, and is an essential consideration in drug formulation and patient care.

The pharmaceutical industry uses advanced formulation techniques, chemical modifications, alternative dosage forms, and absorption enhancers to improve the bioavailability of drugs with poor water solubility or absorption. These innovations help ensure patients receive effective therapy even with challenging drug molecules. Alternative injections, oral dosage forms, such as liquid formulations, orally disintegrating tablets that reduce particle size, pill size modification, chewable tablets, and transdermal patches, are all designed to minimize the difficulty taking pills [2-5].

Importantly, pills and capsules can sometimes pass through the digestive system intact and expelled in the stool. The pharmaceutical industry calls these "ghost pills or capsules." They claim these occur because of extended-release formulations, where many pills and capsules are designed with special coatings or shells that control the release of the medication over time. The outer shell may not dissolve completely and can pass through the gastrointestinal tract, appearing whole in the stool. The general claim is that the active drug was released as intended for most extended-release medications, and only an empty shell is expelled [6,7]. However, no uniform proof exists that the pills or capsules dissolve properly and rapidly transit through the gut.

Low stomach acidity and certain medical conditions may also prevent them from breaking down as planned. Furthermore, not taking a pill with adequate water or food may affect dissolution.

All of the above issues can be addressed by utilizing the NutraNanoSphere (NNS) technology, which is described in this paper with examples of its application.

To demonstrate the importance of NNS technology, we have selected three medical applications that highlight its profound impact in medical research, including cognitive development, malaria treatment, and cancer treatment. We show that NNS Choline may significantly affect cognitive brain development by allowing it to cross the blood-brain barrier. A second medical application of NNS is using four water-soluble NNS molecules to cure malaria in babies. Finally, our early discovery of what is now known as the Natural Killer Cell (NKC) and our early discovery of what are called Cancer Stem Cells (CSCs) demonstrate the importance of the NNS for bioavailability and accessibility. NNS Vitamin C or NNS Curcumin can enter the cancer stem cells intact and dramatically kill the cancer stem cells after their penetration. Finally, the importance of plant botanicals will be demonstrated to highlight their role in targeting CSCs that are not affected by current classical cancer treatment methods.

Materials and Methods

NutraNanoSpheres (NNS). The micellar solutions offer enhanced bioavailability and stability of active substances, enabling efficient product delivery and formulation without compromising sensory or physiological properties. The organic or biological substances are encapsulated in the NNS using proprietary reagents and procedures. The NNS is typically produced in 3-25 nm diameter spheres of uniform size with polydispersity in the 0.01-0.20 range, depending on the inclusion of multiple substances in the same NNS. Stability was measured in years at room temperature.

Cell Line and Media Production: Experiments were performed using a Chronic Myelogenous Leukemia K-652 stem cell line purchased from the American Type Culture Collection (ATCC).

The tissue culture media were made by adding 5 mL of 100X penicillin-streptomycin (10,000 units penicillin with 10 mg of streptomycin/mL—Sigma- Aldrich), 5 mL of 200 mM sterile-filtered L- Glutamine (Sigma-Aldrich), 5 mL of sodium 100X bicarbonate solution (Cellgro), and 50 mL of fetal calf serum (Atlanta Biologics) to 500 mL of Minimum Essential Media, Alpha 1X, withEarle's salts without ribonucleotides, deoxyribonucleotides, and L-glutamine (Cellgro).

Viability Stain: The viability stain used for analysis with the flow cytometerwas developed by Dr. Jerry Thornthwaite. The viability stain, which utilizes a special medium and dye exclusion with Propidium Iodide (Sigma-Aldrich), was effective in measuring cell viability by showing a linear decrease in viability as the K562 cells are progressively subjected to a 56°C water bath over time (data not shown). Additionally, K562 cell viability was measured directly from cell cultures, where 100 µL samples from the cell culture were added to 100 µL of the viability stain. After incubation for five minutes at room temperature, the samples were suspended and analyzed on the Accuri Flow Cytometer (BD Biosciences). Forward Light scatter is used to gate on the K562cells and analyze the number of viable cells within the established control viability gate in the 585 ± 20 nm PI emission red channel. Typical control cultures with 95% to 99% viability were used to establish the boundary of the live cells, which allowed the isotonic PI viability stain to bind the outer cell membranes of the target K562 cancer cells in an isotonic medium, resulting in weak background staining. When the nutraceuticals kill the cancer cells, the compromised cancer cell membranes allow the PI to penetrate the dying or dead cells with significant PI binding nucleic acids, causing a dramatic fluorescence increase as seen in higher fluorescent channel numbers.

Reagents: The highest chemical grades (97%-99%) of Curcumin and Vitamin C, as well as Choline, were used in these studies (Sigma-Aldrich). The "free" Curcumin without being in the NNS was prepared in 100X concentrations of pure Dimethyl Sulfoxide [DMSO] (Sigma-Aldrich) and diluted by a factor of 100 to maintain Curcumin solubility in the cell culture media without DMSO affecting the cancer cell viability.

Encapsulated Reagents: All NNS preparations were manufactured by MiVital, St. Galen, Switzerland.

Average Diameter Measurements of the NNS: The NNS neutraceutical reagents were diluted by volume in a 1:6 ratio with DI Water and filtered through a 0.45 µm Nylon membrane to remove dust contaminants. The Zetasizer ZSP (Malvern Instruments) was used with a backscattering angle of 173 degrees to measure particle size by dynamic light scattering. A non-negative least squares algorithm was used to generate the size distribution by intensity, which indicates the diameter of the significant population for the NNS nutraceuticals. The intensity data was then converted to a mass or volume distribution to compare relative amounts of each size population, which indicated the percentage of the samplerepresented in the respective population. All samples were analyzed at the standards laboratory, Dr. William Brent, Particle Characterization Laboratories, Novota CA.

Sample Preparation and Cell Counting: In all assays, viable cell counts are obtained by mixing 100 µL of cell culture with 100 µL of viability stain and placing the mixture in an ice bucket. All samples were analyzed immediately after ice bath incubation for atleast 5 min. The samples were stable on the ice for at least two hours after preparation. Approximately 50 µL of samples were run through the Flow Cytometer at a medium flow setting (200 cells/sec). The percentage of viable cells was calculated from the gates set for total viable cells/mL, dead cells/mL, and the total cells analyzed. The percentage viability was determined by the number of viable cells divided by the total number of viable and nonviable cells, then expressed as a percentage (100%).

Procedures for Sterilization: All reagent samples were sterile-filtered through 0.22 µm filters and diluted with media in a sterile biological safety cabinet.

Cell Growth Plate Preparation: The cells counted were diluted in media to a concentration of 1 × 105 viable cells/mL. A 500 µL portion of the cells was added to each well of the 48-well plate. The plates were incubated in a Forma Scientific CO_2 water-jacketed incubator at 37.2°C for 48 h to allow the cells to enter the exponential growth phase.

Addition of Compounds: After incubation for 48 h, the stock neutraceutical compounds in the same tissue culture media used to propagate the K562 cells were diluted accordingly by a factor of two for up to eight dilutions. A50 µL sample is added to each well, and up to six replicates of each dilution are prepared inthe wells. 50 µL of cell culture media was added to each controlwell. Once finished, every well contained 550 µL. The plates were typically incubated for up to 48 h.

Cell Processing, Staining, and Analysis: Up to six replicates at each concentration, starting with the controls used to set the viability gates, were suspended in 500 µL of a 1:1 mixture of PBS and DMSO, and 100 µL portions were added to 2 mL 96-well analysis tubes. After all samples were added to the tubes, 100 µL of the viability stain was added using an 8-channel multipipette, and the tray wasshaken slightly and incubated for at least 5 min. All samples are analyzed within one hour after storage on crushed ice, following room temperature incubation for at least 5 minutes. The viability-stained cells were stable for at least two h at ice temperature. A 10 µL portionof each sample was run through the Accuri C6 Flow Cytometer (BD Biosciences) using the fluorescence red channel (585 ± 20 nm) at a medium flow setting (200 cells/sec), and the percentage of viable cells was determined by the number of viable cells/mL.

Percentage Cell Viability: Control cells were used to set the forward angle light scatter gate for the entire cell population, allowing cells with less debris to be gated to theleft of the scatter peak. The background fluorescent peak population consisted of viable cells (95% to 97% viable). Any fluorescent cells to the right of the proper baseline of the viable cell population comprised the dead cell population. The percentage of viable cells was determined by dividing the number of cells in the viable fluorescent cell population by the total number of viable and nonviable cells and multiplying by 100%.

Mice: Male, 6- to 8-week-old DBA/2J mice (Jackson Laboratories, Farmington CT) were utilized in primary sarcoma-lung metastasis experiments.

Tumor System

Murine sarcoma tumors were induced by distal leg subcutaneous (sc) injection of 0.1 ml or a 1% (w/v) solution of 3-methylcholanthrene (MCA) suspended in sesame oil.

Tumors appeared 40 to 120 days after the preshaved flank injection site. The tumors characterized for this study were either analyzed directly from the original MCA-induced mice or after being transferred into syngeneic mice.

Transplanted Tumors

Enzymatically dissociated, 90% viable by Trypan Blue, sarcoma cells (5×104/0.1 ml saline) were intramuscularly (IM) injected into the distal leg of each mouse. On various days, the tumor-bearing legs were amputated while the animals were Nembutal anesthetized. For amputation, a clamp was placed across the extremity above the tumor, and the limb was severed with a cautery unit. The skin was then closed with autoclips. Seven days later, the animals were rechallenged with increasing dosages of dispersed, viable sarcoma cells. These mice were termed the preimmunized group because they could delay tumor growth for a significantly longer time after rechallenge compared to nonimmunized mice (data not shown).

The tumor volumes of these preimmunized groups were measured on various days after rechallenge with 5×10^4 sarcoma cells. Nonimmunized mice were used in which a single dose of 5×10^4 sarcoma cells was injected IM into the distal leg. The animals were analyzed on various days after the injection. Additionally, a saline-injected control group was utilized as a control.

Enzymatic Dissociation of Tumor Tissues

Tumors are aseptically removed and minced with scissors and mixed (20 ml/g tumor with 0.25% trypsin (GIBCO) in Dulbecco's phosphate- buffered saline (PBS). With gentle magnetic stirring, a trypsinizing flask was used for 20 minutes at room temperature. Supernatants, containing single cells, were collected through a 70µm rayon filter into a 50-ml centrifuge tube containing 10 ml of fetal calf serum. The cells were washed once in an IEC PR 2 centrifuge (10 min, 200g, 4°C), and the pellet was resuspended in RPMI 1640 (GIBCO) with 25 mM HEPES buffer and 10% fetal calf serum (RPMI).

The cells were counted and diluted to 2×10^6 cells/mL for DNA flow cytometry. A DNA fluorochrome (8) 4', 6-diamidino-2-phenylindole-2HCl (DAPI) (10µg/ml) was combined with a special Nuclear Isolation Medium (9-11) as a DNA-specific stain for all DNA analyses presented. Cell suspensions were stained by adding 1 mL of NIM-DAPI to 1 mL of a sarcoma or lymphoid cell suspension and incubating on ice for at least 10 minutes before analysis. Sarcoma tissues or mouse liver samples (0.1-0.3 g) were teased directly in DAPI-NIM, filtered, and run after a 10-minute incubation on ice.

DNA Flow Cytometric Analysis

Lymphoid cells were stained at a concentration of 1×10^6 cells/ml. Single fluorescent parameter DNA distribution analysis was accomplished using an ICP-22 flow cytometer (Ortho Instruments). The DAPI fluorochrome was excited at 365 nm using a UG1 filter, with resulting fluorescence measured at 450 nm using a LP410 nm filter. Approximately 2-5×10^6 DAPI-stained nuclei were measured for each experimental determination.

Data Analysis

The data collected were then graphed using PSI-Plot. The data were graphed as percentage inhibition vs. concentration of each component. To calculate percentage inhibition, the values for the viable cells/mL were incorporated into the equation, % Inhibition = (1-X/Y) * 100%, where Xis equal to the cells/mL in a particular well, and Y is the average number ofcells/mL in the control. The mean of multiple replicates (4-6) ± the Standard Deviation (SD) is then determined.LD50 is the concentration, either in nmol or µmol per well, of the supplement of interest that causes 50% cell death. For DNA analysis, the peak channel and coefficient of Variation were determined.

Malaria Treatments

We have developed a cure for malaria, which has been approved by the Ministers of Health in Nigeria and Haiti. To treat malaria in adults and children, we used a combination of Curcumin, Artemisinin, and Citrus Bioflavonoids in gel caps, administered over 16 days [27-39]. To treat babies, we had to use the NNS oral dose [30,31]. Therefore, each component was formulated into the NNS form (28.1 nm diameter and 0.111 polydispersity) with a combination of Curcumin, Artemisinin, Bilberry, and Vitamin D3. The daily dosage of the NNS malaria treatment, TriAntiVPTM, consisted of 0.5 mL of each dosage containing 25 mg of Curcumin, 25 mg of Artemisinin, 25 mg of Bilberry, and 900 IU of Vitamin D3. 0.5 mL of TriAntiVP was added to 30 mL of milk and administered to the baby using a baby bottle. The malaria dosage and malaria counts were done every day for 16 days. The Mean Parasite Load (MPL) was measured from Day 0 through Day 16 and again at Days 30 and 60 after treatment.

Results

Micelle Structure

The structure of a micelle and the resulting sphere products are shown in figure 1.

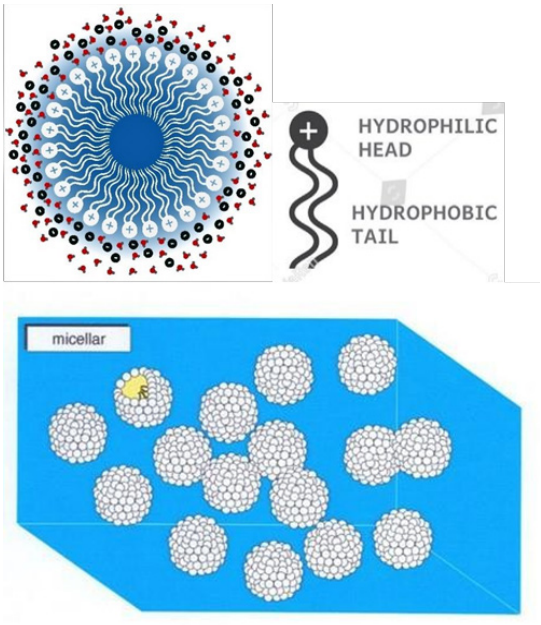

Figure 1: NutraNanoSpheres with the hydrophilic head (water-soluble) and internalized hydrophobic tail, making a perfect sphere housing the nutraceutical of choice.

For example, the micellation of 6% curcumin results in a bioavailability of the Curcumin in the bloodstream many times better than the so-called "free form" of Curcumin in tablet form. The concentration of the Curcumin NNS is over 4.5×10^{18} micelles/mL. The average diameter is 7 nm. A natural fatty acid, an energy metabolite, encapsulates molecules in nanosized "micelles" in which over 1000 of them would stretch across a human red cell. The small size is critical for the NNS's increased bioavailability and long-term stability. The Hydrophilic (water-loving) and the Hydrophobic ("water-fearing") hydrocarbon parts of the fatty acid spontaneously form the micelle. No organic solvents or elevated temperatures were used in our natural "entrapping" our nutraceuticals in the micelles. This process enables us to achieve high bioavailability and potency of our nutraceuticals. The NNS are stable up to 98°C and can be stored at room temperature for years.

The importance of the size of the micelle versus stability is shown in Figure 2. The lower right quadrant shows the range of diameters we experience for most of the NNS preparations, yield years of stable NNS. Compare the micelles on the market, which range from being stable for months to seconds.

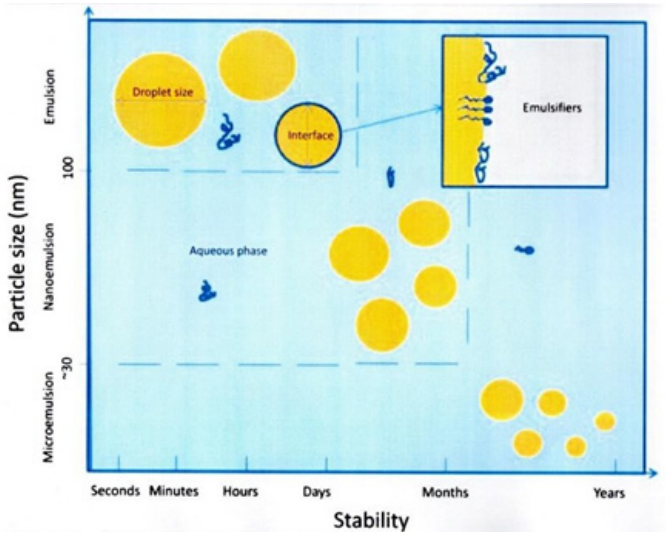

Figure 2: (Diagram from Malvern Instruments). Scatter diagram illustrating the comparison between the stability of micelles and their size. Therefore, it is important to make the NNS within the stable range of 3-50 nm.

The following figures illustrate the high-resolution nature of the NNS. For example, Figure 3 compares the NIST (National Institute of Standards and Technology) standard tracer, a finely prepared carbon particle, and the Zeta Sizer dynamic light scatter sizing instrument (Brookhaven Instruments). Figure 3 shows the dynamic backscatter data for the 101 nm NIST standard versus the biologic sample of NNS Vitamin D3, which shows a decent comparison in polydispersity.

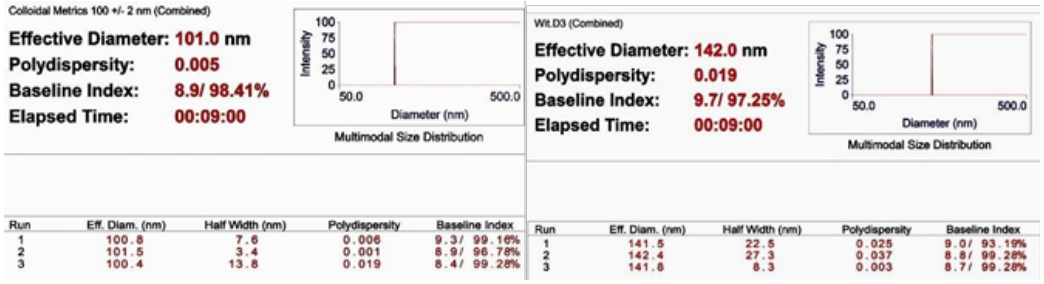

Figure 3: Comparisons between the NIST 101nm Standard and NNS Vitamin D3.

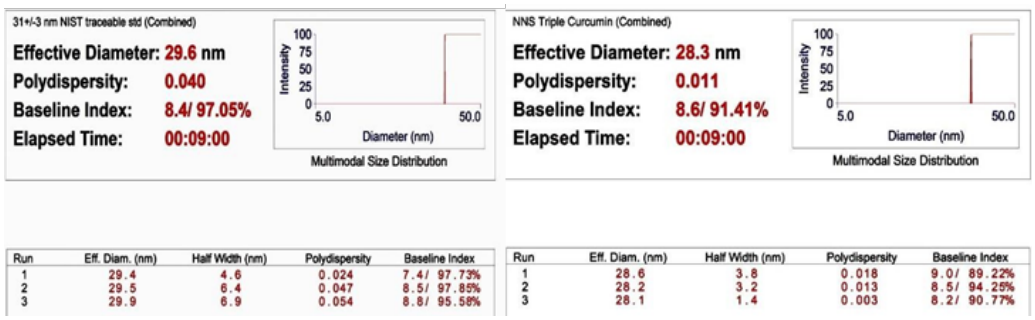

Figure 4: Comparisons between the 31nm NIST Standard and NNS Triple Curcumin.

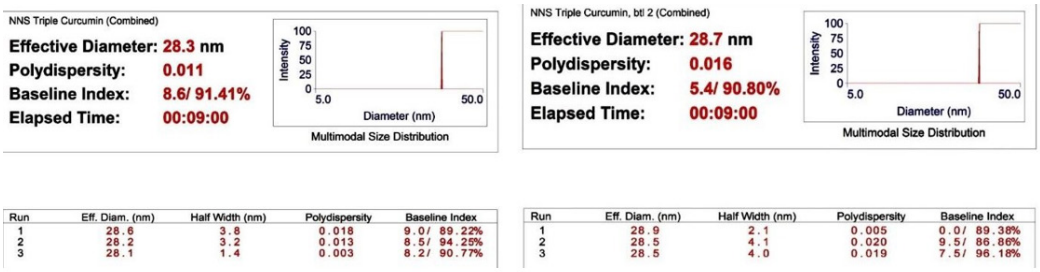

Figure 5: Precision of a duplicate measurement of Triple Curcumin.

Figure 4 presents the quality of the NNS samples as shown by the comparison of the 31nm NIST Standard and what is called Triple Curcumin. The Triple Curcumin contains the three naturally occurring Curcuminoids with their relative distributions. These natural distributions contain Curcumin (70-80%), Demethoxycurcumin (15-20%), and Bisdemethoxycurcumin (1-3%), thus the name Triple Curcumin. The polydispersity distribution of the Triple Curcumin is about four times better than the NIST standard.

Figure 5 shows the precision of the dynamic light scattering measurement for Triple Curcumin. The average diameter of pure Curcumin (97%) is 7.4 nm.

There are numerous examples of how NNS can encapsulate a wide range of molecules. Briefly, we can combine different NNS to create, for example, Heart, Brain, Antidepressant, and Energy formulations, to name a few. For example, the Energy Formulation consists of Curcumin, Vitamin C, Ginger, and Siberian Ginseng (27.8nm diameter with a 0.058 polydispersity) for the Asian market. The NNS products can withstand 178°C for 30 sec., the sterilization process in the energy drink business, thus enabling them to fit seamlessly into production. Virtually any NNS product can be converted into a time-release formulation, allowing for single, double, or triple coating. Combining these different-sized coatings makes for a time-release formulation that lasts for hours. For example, a single-coated Vitamin C has an average diameter of 5.25 nm, while the triple-coated version is 43.0 nm, which enables an eight-hour time-release formulation.

To demonstrate the significance of the NNS technology, we have selected three medical applications that highlight the profound impact of our medical research on cognitive development, malaria prevention, and cancer treatment. As examples, we show three applications: one using a single molecule, Choline, that affects cognitive brain development by allowing it to cross the blood-brain barrier, another using four NNS in the same preparation to cure malaria in babies, and final two examples to show the importance of the NNS for bioavailability and accessibility where NNS Vitamin C or Curcumin enters the cancer stem cell intact and show a dramatic ability to kill the cancer stem cells. A presentation of our early discovery of what is now called the Natural Killer Cell (NKC) and the Cancer Stem Cells (CSCs). Finally, the importance of plant botanicals, illustrated by Curcumin and Vitamin C, is presented to demonstrate their potential in killing CSCs that are not affected by the current, classical cancer treatment methods.

Application of NNS Choline in Cognitive Treatments

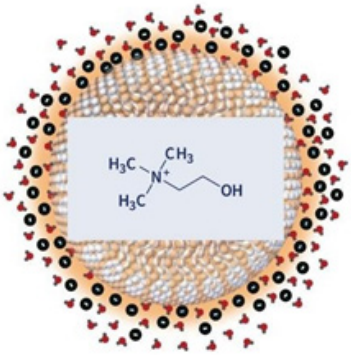

Figure 6: NutraNanoSphere encapsulates Choline, enabling its passage across the blood- brain barrier. The NNS Choline has an average diameter of 8.3nm with 0.256 polydispersity.

Choline (2-hyroxy-N,N,N-trimethylethanamium) is an essential nutrient for humans and many other animals [12]. The cholines are a family of water-soluble quaternary ammonium compounds [13,14]. Choline is the parent compound of the choline class, consisting of ethanolamine having three methyl substituents attached to the amino function [15].

Choline uptake into the brain is controlled by a low-affinity transporter at the blood-brain interface[16]. Transport occurs when arterial plasma choline concentrations increase above 14 µmol/l, which can occur during a spike in choline concentration after consuming choline-rich foods. A standard 1.0 ml dosage of 10.0% NutraNanoSphere™ Choline is determined (see below) to be 320 µmol, at least 23 times greater than the initial transport of Choline across the blood-brain barrier.

Neurons acquire Choline from both high- and low-affinity transporters. Choline is stored as membrane-bound phosphatidylcholine, which can later be used for acetylcholine neurotransmitter synthesis. Acetylcholine is formed as needed, travels across the synapse, and transmits the signal to the neurons. Afterward, acetylcholinesterase degrades it, and the free Choline is taken up by a high-affinity transporter into the neuron again [17].

Current scientific studies suggest that Choline may improve memory and cognition and reduce the risk of ischemic stroke. Choline supports brain development and growth in newborn babies, significantly decreasing the risk of neural tube defects (NTDs) [18]. Both pregnancy and lactation increase the demand for Choline dramatically. This demand was met by the upregulation of phosphatidylethanolamine-N-methyltransferase (PEMT) via increasing estrogen , which also suggests that Choline may reduce the risk of preeclampsia and congenital irregularities. Choline is required to produce acetylcholine ,a neurotransmitter, and S- adenosylmethionine (SAM), a universal methyl donor. Upon methylation, SAM is transformed into homocysteine [19].

Choline is in high demand during pregnancy as a substrate for building cellular membranes (rapid fetal and mother tissue expansion), increasing the need for one- carbon moieties (a substrate for methylation of DNA and other functions), raising choline stores in fetal and placental tissues, and for increased production of lipoproteins (proteins containing "fat" portions) [20-23]. In particular, there is interest in the impact of choline consumption on the brain. This stems from Choline's use as a material for making cellular membranes (particularly in making phosphatidylcholine). Human brain growth is rapid during the third trimester of pregnancy and continues to be fast for approximately five years [24]. The demand for sphingomyelin, made from phosphatidylcholine derived from Choline, is high during this time. Because this material is used to myelinate (insulate) nerve fibers [25], Choline is also in demand for the production of the neurotransmitter acetylcholine, which can influence the structure and organization of brain regions, neurogenesis, myelination, and synapse formation. Acetylcholine is present in the placenta and may help control cell proliferation, differentiation, and parturition [26]. When Choline concentrations in the plasma increase above 14 µmol/liter, transport into the brain occurs. A 1.0 ml dosage of 10% Choline. Therefore, our current Choline is 10.0% or 100 g/liter or 100g/1000 ml = 0.1 g per 1ml dosage or 100mg. 100mg/1.0 ml of 10% Choline, assuming 100% bioavailability, would yield 100 g Choline/10^4.17 g/mole of Choline = 0.96 mol/liter of plasma, assuming 100% bioavailability. There are 3 liters of plasma in the human body. Therefore, a 1.0 ml dosage of 10% Choline could be theoretically diluted in an average of 3.0 liters of adult plasma as the worst-case scenario for dilution. This value is probably much less because of the NNS's ability to deliver on a nanoscale. Using the 3.0-liter dilution, the concentration of Choline in the plasma would be (0.96 mol/liter divided by 3.0 liters = 0.32 mol/liter). To get the number of moles in one ml of a dosage of 10% Choline, one would divide 0.32 mol/liter x 1 liter/1000ml = 3.2 x 10^{-4} moles per liter dosage or 320 µM. Divide 320µM/14µM = 22.9 times higher than needed to initiate transport across the blood-brain barrier by Choline. Therefore, a 1ml dose of 10% Choline could easily be transported across the blood- brain barrier.

Application of NNS antimalaria treatments in Babies

We have developed a cure for malaria, which has been approved by the Ministers of Health in Nigeria and Haiti for curing malaria in adults and children. A combination of Curcumin, Artemisinin, and Citrus Bioflavonoids in gel caps has been administered over 16 days with success in 90% of children and 100% of adults [27-30]. To treat babies [31,32], we had to use the NNS water-soluble oral dose. Therefore, each component is made into the NNS form for Curcumin, Artemisinin, Bilberry, and Vitamin D3. The NNS malaria treatment was called TriAntiVP™, which denotes its use as an antiviral and antiparasitic nutraceutical formulation. It consists of 0.5 mL containing 25 mg of Curcumin, 25 mg of Artemisinin, 25 mg of Bilberry, and 900 IU of Vitamin D3. The NNS average diameter was 28.1nm with an excellent polydispersity of 0.111. 0.5ml of TriAntiVP™ was added to approximately 30ml of milk and administered to the baby using a baby bottle every day for 16 days. The Mean Parasite Load (MPL) was measured from Day 0 through Day 16 and again at Days 30 and 60 after treatment. Table 1 shows the success of eradicating malaria, where 93% (60 days, n = 15) of the babies were cured [31].

Table 1

Water Soluble NutraNanoSphere™ TriAntiMal™

Proprietary Formulation for Babies

93.3% Cured through Day 60 (n = 14)

LAB NO	Age(mo.)	Sex	MPL 0	MPL 1	MPL 2	MPL 3	MPL7[4]	MPL10	MPL16	MPL 21	MPL 30	MPL 60	REMARKS
PF/021[1]	24	Female	7240	3160	1680	760	0	0	0	0	0	0	completed
PF/023	24	Male	5120	2840	760	0	0	0	0	0	0	0	completed
PF/024	12	Male	6440	3720	520	0	0	0	0	0	0	0	completed
PF/025[2]	12	Female	7640	4680	2120	320	0	0	0	0	0	0	completed
PF/027	14	Female	6480	2920	760	0	0	0	0	0	0	0	completed
PF/028	10	Male	9320	4200	1960	360	0	0	0	0	0	0	completed
PF/029	24	Female	7240	3960	1720	0	0	0	0	0	0	0	competed
PF/030	36	Male	10120	7840	3360	520	0	0	0	0	5280		Failed
PF/31	24	Male	3160	720	0	0	0	0	0	0	0	0	completed
PF/32	15	Female	4840	2160	400	0	0	0	0	0	0	0	completed
PF/33	24	Female	6560	2920	840	0	0	0	0	0	0	0	completed
PF/34[3]	12	Female	7120	3760	1020	0	0	0	0	0	0	0	completed
PF/37[3]	9	Male	4120	2000	760	0	0	0	0	0	0	0	completed
PF/39	24	Female	3120	1440	680	0	0	0	0	0	0	0	completed
PF/40	35	Female	4280	2440	760	0	0	0	0	0	0	0	completed
Mean	**19.9**	**Male**	**6187**	**3251**	**1156**	**131**	**0**	**0**	**0**	**0**	**352**	**0**	
SD	**8.7**	**40%**	**2074**	**1658**	**858**	**243**	**0**	**0**	**0**	**0**	**1363**	**0**	

[1]PF/22 out of study; never started [2]PF/26 successfully completed 16 Day treatment but was lost to follow-up [3]PF 35.36.38 Lost to Follow-up
[4]MPL clearance was 100% (15/15) by Day 7

From ref [31].

In TABLE 1, the MPL decreased to zero for all 15 babies by day 7, while the lone positive reoccurred at Day 30. The resulting cure rate was 93.3% for babies with an average age of 19.9 months.

Application of NNS treatments for destroying Cancer Stem Cells (CSC)

During the early 1970s, we made two specific discoveries that helped shape our cancer therapeutic approaches.

Our First Discovery was understanding the fundamental process of metastatic disease. We used a chemically induced cancer model by painting the shaved distal thigh musculature of DBA/6J mice with 1.0% 3-methylcholanthrene in sesame oil. About 90% of the mice would develop an intramuscular tumor on site within six months. The original chemically induced cancer cells were enzymatically dissociated into single cells, and 5 × 104 sarcoma cells in 0.1 ml were injected intramuscularly into new mice. Using our DAPI-Nuclear Isolation Medium (9) and our high-resolution DNA flow cytometry (10,11), we produced DNA histograms of the tumor cell populations.

When the primary tumors reached 2.0 cm in diameter, we could see the metastatic nodes develop in the lungs using an India ink contrast stain. This enabled us to dissect about 10 small 1.0 mm metastatic nodules and enymatically dissociate the metastatic cancer cells into viable populations, as described above. The metastatic tumors were almost exclusively diploid, showing a normal total DNA content. The diploid metastatic tumors were transplanted (5 x 104 cells) intramuscularly. As the diploid tumors were allowed to grow significantly, a population of both diploid cancer stem cells (CSCs) and aneuploid or so-called heteroploid cancer cells would develop. Therefore, the metastatic lung cancers would be all diploid CSCs with a small S-phase population undergoing division. Also interestingly, if these metastatic diploid cells are injected intradermally, they grow as an aneuploid population containing both diploid cancer stem cells and aneuploid daughter cancer cells with the same DNA Index (mean DNA channel of aneuploid peak divided by the mean channel of the diploid channel by DNA flow cytometry), which was a fingerprint for each unique tumor. We could repeat this process many times. Our early observations revealed the diploid population of an aneuploid cancer was the most virulent to metastasis. The diploid metastatic CSCs would have a good chance of escaping the immune system, as their cell surfaces would appear normal. They would be less affected by chemotherapy or radiation therapy because of their low S-phase. The standard modalities of treatment have focused on destroying daughter cancer cells while having minimal effect on the CSCs. The details of the underlying cause of metastases in our sarcoma model will now be presented.

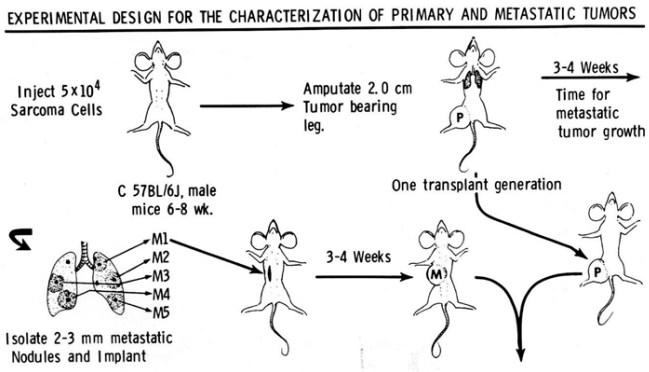

Figure 7: Experimental Design for the Characterization of Primary and Metastatic Tumors.

Figure 7 shows the general scheme of our study of metastasis in a chemically induced sarcoma model. The basic finding was that chemically induced aneuploid (also termed heteroploid) sarcomas metastasize as diploid metastatic tumors.

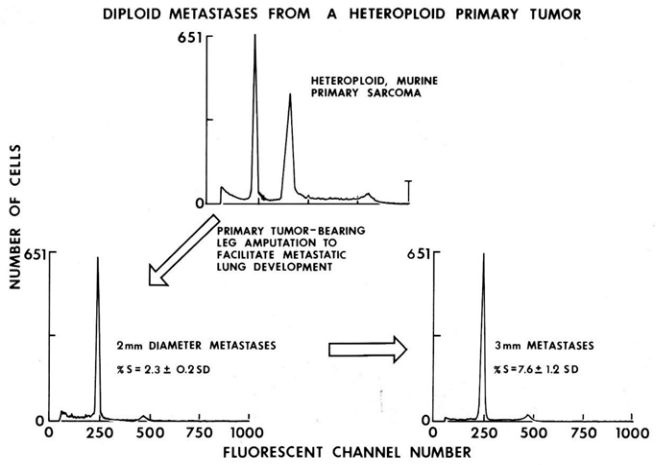

Figure 8: Diploid Metastases from a Heteroploid (Aneuploid) Primary Tumor.

In the mouse model shown in Figure 8, the resulting lung metastatic disease was identified as diploid. This makes sense because the cancer stem cells (CSC) want to present themselves as being as normal as possible. A diploid CSC would appear more normal without significant DNA alterations of cell surface proteins. Furthermore, the low S-phase of these cells would show minimal if any susceptibility by DNA targeted chemotherapeutic or radiation treatments. Our discovery that aneuploid tumors metastasize as diploid tumors has profound significance in understanding how CSCs function to establish themselves as distant metastases.

As the primary tumor grew, metastases developed in the lungs. The growth of metastases is enhanced by the surgical removal of the primary tumor, as shown in Figure 8. The reason for this was not apparent, but it could be that the primary was sending a signal to the metastatic lung metastases, controlling their growth. In a way, it may make sense that the primary cancer did not want to destroy its host. A similar human example can be seen when a primary tumor is removed, and a phenomenon called "Tumor Flare" results, where metastatic disease spreads rapidly after the primary tumor is removed. Perhaps the whole concept of trying to remove the primary tumor as the first step in cancer therapy should be reevaluated. Natural Killer Cell (NKC)/ CSCs protocols using NNS nutraceuticals could possibly be implemented immediately before surgery occurs. Frequently surgery is delayed for weeks to allow for scheduling. The immediate treatments would allow the *in situ* NKC and CSCs NNS reagents to start destroying the primary and any micro-metastatic disease, which are not treatable by current medical protocols.

Figure 9 shows the diploid nature of the metastatic nodules. Metastatic nodules as large as 9mm in diameter maintain their metastases' diploid nature.

Diploid metastatic lung nodules will result in the same DNA Index (ratio of the mean DNA peak channel of the aneuploid population over the mean DNA peak channel of the diploid population) whether transplanted *in vivo* or passed in culture. Multiple passages [5-10] of the cancer cells will result in the loss of the diploid population (Figure 10). Interestingly, the DNA Index remains constant for each chemically induced tumor. Each chemically induced tumor also develops its unique DNA Index, which remains the same throughout many passages. We have seen this happen many times. REF.

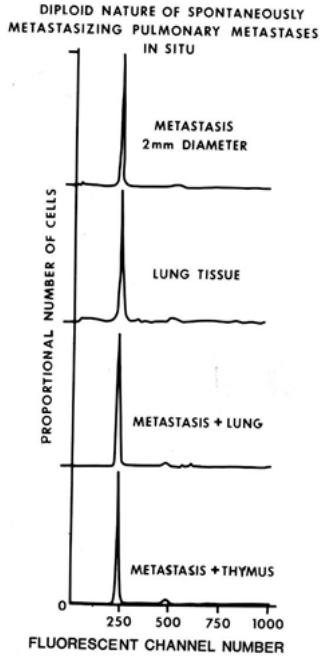

Figure 9: DAPI-NIM DNA Histogram showing that the metastatic nodules are diploid compared to normal lung and thymus tissues.

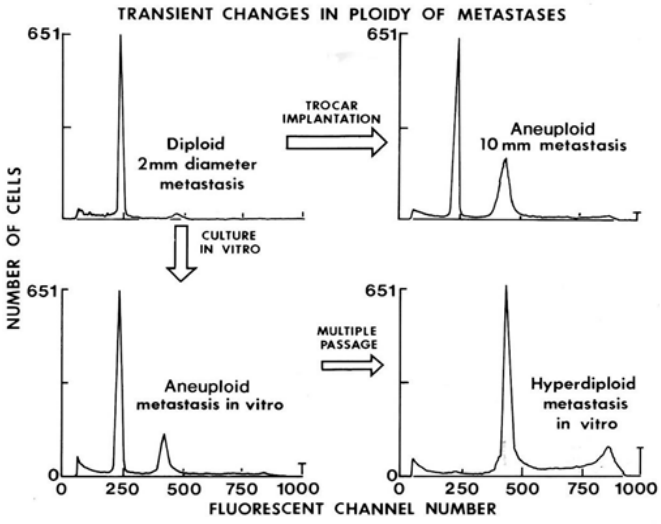

Figure 10: Transient Changes in Ploidy of Metastases. Diploid Metastases are enzymatically dissociated and put in culture or Trocar-implanted under the flank skin as a whole nodule in a new mouse.

When a metastatic lung lesion reaches a significant size, one can observe the beginning of its aneuploid population developing, even though only a very small percentage of aneuploidy (less than 5%) is initially detected. In Figure 11, the DNA Index equals the

channel 387aneuploid peak divided by the channel 219 diploid peak, which equals 1.77. The DNA Index is like a fingerprint for each chemically induced sarcoma. The DNA Index was constant for each tumor regardless of the number of passages *in vitro* or *in vivo*.

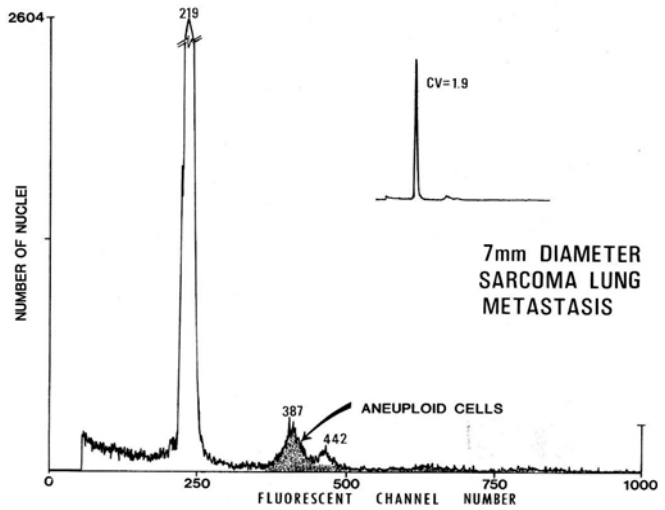

Figure 11: A 7mm lung metastasis DNA histogram shows a low percentage of aneuploid cells.

Table 2 Ploidy Values obtained from DNA Histogram analyses of DAPI-stained nuclei isolated from primary and Metastatic Sarcoma Tissues

Origin of Tissues	Number Studied	% Aneuploid Nuclei
Primary Sarcoma	14	63.1 ± 4.0
Primary after Passage in Cell Culture	10	87.9 ± 4.1
Excised Lung Metastases	25	1%
Lung Metastasis transplanted Subcutaneous in a New Mouse	14	44.1 ± 9.4
Lung Metastases after passage in Cell Culture	5	55.1 ± 18.0

Values are Mean ± SD

Table 2 shows the high degree of aneuploidy that results when a sacrcoma develops on each flank of mice after painting the skin with a carcinogen. The Primary sarcomas even at 2 mm in diameter contained aneuploid cells. All excised lung metastases between 2 to 8mm in diameter maintained their diploid DNA histogram pattern where aneuploidy was only 1%. The diploid metastases, after enzymatic single cell preparations, were either transplanted into the flank of a new mouse or placed in cell culture. Aneuploid cells started growing out of the diploid cell populations resulting in the same DNA Index as the original chemically induced sarcoma. These data show the cancer stem cells (CSCs) originate in the diploid portion of primary aneuploid sarcoma because only these diploid cells have the ability to evade the immune system and establish themselves as diploid lung metastases. The diploid CSCs still had the capacity to transform into daughter aneuploid cells as we showed [32] in 1979.

Our **Second Discovery** earlier in 1972 was observing that sheep erythrocytes [33-35] and, later, CSCs [36] are spontaneously destroyed by circulating lymphocytes without prior immunization. These lymphocytes, subsequently called Natural Killer Cells (NKC), are the first line of defense in the blood against viruses and cancer stem cells. Much of our research has utilized neutraceuticals to enhance the NKC activity against cancer cells.

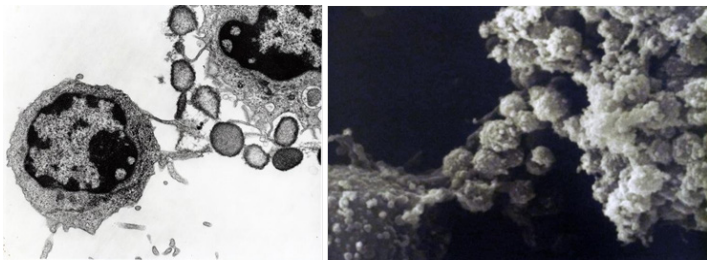

Figure 12: Transmission (left panel) and Scanning (right panel) showing Natural Killer Cell (NKC) releasing its toxins to destroy (blebbing of the cancer cell membranes) the target K562 leukemic stem cell [36].

Normal stem cells are primitive cells that can produce any tissue. During the process of carcinogenesis, normal stem cells can undergo metabolic alteration and become CSCs. The Natural Killer Cells (NKC) can recognize the cell surface alterations and kill the transformed CSCs. Furthermore, natural plant products such as Curcumin, Artemisinin, Genistein, Resveratrol, and Vitamin C can destroy cancer stem cells [37]. However, most conventional cancer treatments do not destroy CSCs. Instead, they kill some of the daughter cells, causing a decrease in tumor size. The drug and radiation-resistant CSCs may lie dormant for years, only to become even more aggressive and resistant to conventional treatment.

The Importance of Bioavailability and, even more importantly, Accessibility

In Figure 13, the percentage of inhibition of in vitro cancer stem cell is shown in duplicate for Vitamin C and Curcumin. No Inhibition in tumor growth was observed with the addition of highly soluble Vitamin C to the tumor cell culture, even at a high concentration of 10,000 µM/10^4 K562 stem cells per well. However, when the NNS Vitamin C was used in culture, the Lethal Dose where 50% of the K562 cancer stem cells were inhibited from growing (LD50) was observed at 125 and 140 µm.

If so-called "free" Curcumin was solubilized in DMSO (Dimethyl sulfoxide) to make it soluble in the cell culture media, a measurable LD_{50} at 11,000 nm was seen. However, if the NNS Curcumin was used, the average LD_{50} was 34 nmol, showing an LD_{50} 324 times more potent than the "free" Curcumin without NNS. We use the term "Accessibility" to describe the importance of the NNS nutraceuticals in their penetration of the target CSCs. While bioavailability is critical to allow survival through the stomach into the bloodstream, more important is the accessibility that enables the NNS to penetrate the target CSC cell membrane and probably even the mitochondria to initiate the killing process more effectively.

Figure 14 shows how quickly the killing of K562 cells occurs. CSC death by exposure to NNS Curcumin is probably instantaneous, as mixing and running on the flow cytometer can delay the analysis by up to 30 seconds. NNS Curcumin does not harm normal cells

and adds to the nutritional nature of curcumin and all of the anti-CSCs nutraceuticals report herein.

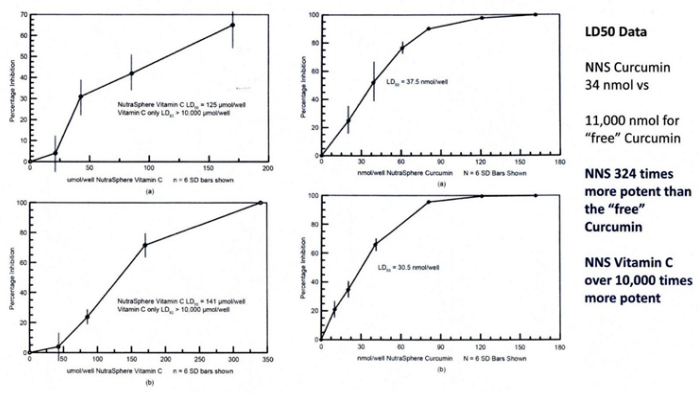

Figure 13: The Percentage of Inhibition of CSC growth of K562 cancer stem cells by NNS Vitamin C and NNS Curcumin [37].

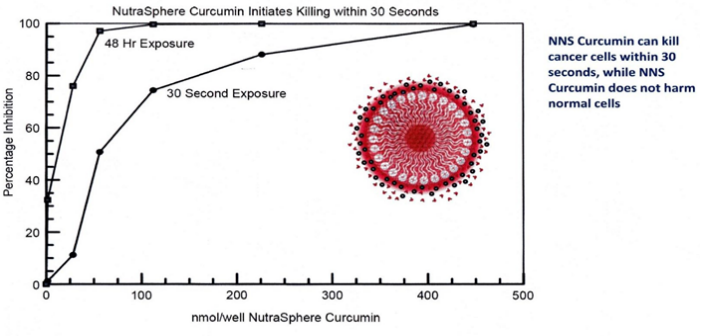

Figure 14: NutraNanoSphere Curcumin initiates killing within 30 Seconds [37].

Natural Products that Kill CSCs

Curcumin and CSCs

Curcumin, a bioactive compound found in turmeric, has been studied for its potential anticancer properties, including its effects on cancer stem cells (CSCs). Cancer stem cells are a subpopulation of cells within tumors that can self-renew and drive tumor growth, and they are often resistant to conventional therapies.

Research has indicated that Curcumin may exert several effects that could be beneficial in targeting cancer stem cells. Curcumin can inhibit the self-renewal and proliferation of cancer stem cells, reducing their ability to contribute to tumor growth and metastasis in human breast [38] and colon [39] cancers. Curcumin can kill CSCs by inducing apoptosis, modulating signaling pathways to maintain CSCs, enhancing chemosensitivity to treatment by overcoming resistance, and providing anti-inflammatory and antioxidant effects. Therefore, targeting CSCs is a significant area of research in cancer therapy, as these cells are often responsible for tumor recurrence and resistance to conventional treatments.

Natural products have been a rich source of potential anticancer agents, including those that may target CSCs. Research into the effects of various natural compounds on CSCs is ongoing, and while many studies are still in preclinical stages, some natural products have shown promise in this area [38-41]. Indeed, from our research, we have seen the ability of NNS Curcumin and Vitamin C to kill CSCs *in vitro* [37] effectively. Here are several natural products that being investigated for their potential to kill or inhibit CSCs [39]:

Curcumin

1. **Induction of Apoptosis**: Curcumin is shown to induce apoptosis (programmed cell death) in various cancer cell types, including CSCs. It can activate intrinsic apoptotic pathways by increasing the expression of pro-apoptotic proteins (like Bax) and decreasing anti-apoptotic proteins (like Bcl-2). [42-45]
2. **Inhibiting Angiogenesis**: Curcumin can alter the tumor microenvironment by inhibiting angiogenesis (formation of new blood vessels) and reducing the recruitment of inflammatory cells. A less supportive microenvironment can hinder the growth and maintenance of CSCs [46-49].
3. **Inhibition of Drug Resistance**: CSCs are often associated with resistance to conventional chemotherapy and radiotherapy. Curcumin has been reported to downregulate the expression of drug efflux pumps (like ABC transporters) and enhance the sensitivity of CSCs to chemotherapeutic agents [50,51].
4. **Inflammation Elimination**: Cancer progression is associated with chronic inflammation and the maintenance of CSCs. Curcumin has anti-inflammatory properties and can inhibit the expression of pro-inflammatory cytokines and enzymes (like COX-2 and NF-κB), which may contribute to the survival and proliferation of CSCs [52-54].
5. **Reactive Oxygen Species (ROS) Generation**: CSCs often have enhanced antioxidant defenses. Curcumin can induce oxidative stress in cancer cells, leading to cellular damage and death [55-58].
6. **Inhibition of CSCs Signaling Pathways**: Curcumin can inhibit key signaling pathways that secure the continual function of CSCs. These pathways include the Hedgehog, Wnt/β-catenin, and Notch pathways. The disruption of these pathways with Curcumin reduces the tumorigenicity and self-renewal capacity of CSCs [59-63].
7. **Epigenetic Mechanisms to Silence Oncogenes**: Curcumin can modify epigenetic mechanisms, such as DNA methylation and histone modification. These changes can lead to the re-expression of tumor suppressor genes and the silencing of oncogenes, thereby inhibiting the behavior of CSCs [64-68].
8. **Cell Cycle Regulation Interference**: Curcumin can affect cell cycle progression by modulating the expression of cyclins and cyclin-dependent kinases (CDKs), leading to cell cycle arrest in CSCs and preventing their proliferation [69-72].
9. **Metabolic Pathway Alteration**: Curcumin can target the metabolic pathways of CSCs, shifting CSCs' metabolism from oxidative phosphorylation to glycolysis, affecting their survival and proliferation [73-76].

Vitamin C

Cancer Stem Cells (CSCs) are self-renewing, multi-potent cells responsible for tumor recurrence, metastasis, chemoresistance,

and heightened mortality. Vitamin C can selectively target CSCs via epigenetic and metabolic pathways in various cancers [77]. Vitamin C selectively targets multiple cancer cell types at high doses (10-20 mM in human plasma) through its prooxidant action, while at low doses (40-80 μM), it enhances antitumor immunity by acting as an antioxidant. This versatility makes Vitamin C a promising antitumor agent for standalone and combination therapies [78,79]. Specific doses of vitamin C can stop cancer cell glycolysis and block nitroso synthesis, indicating the potential of vitamin C in cancer treatment. The Program Death Ligand (PD-L1) is often expressed on the surface of cancer cells, inhibiting T cell activation, thus allowing cancer cells to evade the immune system [80]. Recent studies have revealed that Vitamin C enhances the cancer's immune response to anti-PD-L1 therapy through multiple indirect approaches [81]. Vitamin C is essential in generating and maintaining normal stem cells [82].

Resveratrol

This polyphenolic compound, derived from grapes and berries, has been shown to inhibit the proliferation of cancer stem cells in various cancers, including breast and colon cancer, by inducing apoptosis and inhibiting key signaling pathways. Resveratrol is a potent reducing agent and can prevent carcinogenesis due to its antioxidant abilities [83]. A significant challenge in treating cancer is the development of drug resistance, which can result in treatment failure and tumor recurrence. Targeting CSCs and non-coding RNAs (ncRNAs) with Resveratrol can combat this problem by lowering cancer drug resistance and opening up new therapeutic options.

Resveratrol alters the expression of genes related to self-renewal, modulating essential signaling pathways involved in cancer initiation and CSC control. Additionally, Resveratrol affects non-coding RNAs (ncRNAs) [84]. Wnt/β-catenin signaling is a crucial pathway in various cellular processes, including cell proliferation, differentiation, and migration. Lithium chloride (LiCl) is known to activate this pathway by inhibiting glycogen synthase kinase 3 beta (GSK-3β), an enzyme that typically promotes the degradation of β-catenin. When GSK-3β inhibited, β-catenin accumulated in the cytoplasm and translocated to the nucleus, where it can activate Wnt target genes. Resveratrol treatment attenuated the activation of Wnt/β-catenin signaling by LiCl (GSK3β agonist) [85]. Resveratrol also reversed IL-6-promoted lung CSCs properties and Wnt/β-catenin signaling. Therefore, Resveratrol inhibits lung cancer by targeting Lung CSCs and IL-6 in the tumor microenvironment. The novel findings from this study provided evidence that RES exhibited multi-target effects on the suppression of lung cancer and could be a novel potent cancer-preventive compound [86]. Since current cancer therapies fail to eradicate CSCs, leading to cancer recurrence and progression, targeting of CSCs with phytochemicals such as Curcumin, EGCG, sulforaphane, Resveratrol and Genistein, combined and/or in combination with conventional cytotoxic drugs and novel cancer therapeutics, may offer a novel therapeutic strategy against cancer [87].

ECGC

Green tea is among the most popular beverages globally, especially in Asian countries. Consumption of green tea is demonstrated to possess many health benefits, which are mainly attributed to the main bioactive compound epigallocatechin gallate (EGCG), a flavone-3-ol polyphenol, in green tea. EGCG is primarily absorbed in the intestine and gut microbiota, and plays a critical role in its metabolism before absorption. EGCG exhibits versatile bioactivities, with its anticancer effect being most attractive due to the cancer preventive effect [88].

Cancer preventive activities of green tea and its main constituent, (-)-epigallocatechin gallate (EGCG) are reported in a recent review to delay cancer onset as shown by a 10-year prospective cohort study, prevent of colorectal adenoma recurrence in a double-blind randomized clinical phase II trial, and show inhibition of metastasis of B16 melanoma cells in the lungs of mice [89]. Furthermore, Food-derived polyphenols, such as ECGC and Curcumin, can attenuate the formation and virulence of breast CSCs, implying that these compounds and their analogs might be promising agents for preventing breast cancer [90]. EGCG-induced sensitization to 5FU through targeting of CSCs may serve as an adjunctive treatment to conventional chemotherapeutic drugs in colorectal cancer patients [91]. Recurrence following chemotherapy is observed in the majority of patients with pancreatic ductal adenocarcinoma (PDA) due to the CSCs. Phosphodiesterase-3 (PDE3) inhibitors are a class of drugs that inhibit the activity of the phosphodiesterase 3 enzyme, which is responsible for the breakdown of cyclic adenosine monophosphate (cAMP) and cyclic guanosine monophosphate (cGMP). By inhibiting PDE3, these drugs increase the levels of cAMP and cGMP in cells, leading to various physiological effects. An EGCG analog capable of inducing strong cGMP production drastically suppressed the CSC properties of PDA and extended the survival period in vivo. The combination treatment of EGCG and a PDE3 inhibitor as a potent cGMP inducer could be a potential treatment candidate for eradicating CSCs of pancreatic ductal adenocarcinoma [92].

Genistein

Genistein, a soy-derived isoflavanoid compound, exerts anticancer effects in various cancers. Nasopharyngeal cancer stem cells (NCSCs) are a small subpopulation of cancer cells responsible for the initiation, progression, metastasis, and recurrence of nasopharyngeal cancer. The present study aimed to investigate the suppressive effects of Genistein on NCSCs and its underlying mechanism [93]. Genistein effectively inhibits tumor growth and dissemination by modulating key cellular mechanisms. These include the inhibition of epithelial-mesenchymal transition, the suppression of angiogenesis, and the regulation of cancer stem cell proliferation. These effects are mediated through pivotal signaling pathways such as JAK/STAT, PI3K/Akt/mTOR, MAPK/ERK, NF-κB, and Wnt/β-catenin. Moreover, Genistein interferes with the function of specific cyclin/CDK complexes and modulates the activation of Bcl-2/Bax and caspases, playing a critical role in halting tumor cell division and promoting apoptosis. These mechanisms directly affect the survival of the CSCs [94]. Genistein

inhibits Gli1 gene expression, resulting in the attenuation of cancer stem-like properties in gastric cancer cells. In addition, Genistein suppresses the cell invasive capacity required for tumor growth and metastasis. Therefore, Genistein can be an effective agent for gastric cancer therapy by targeting cancer stem-like characteristics [95]. Granulocyte colony-stimulating factor (G-CSF) treats neutropenia in various clinical settings. Although beneficial, there are concerns that the chronic use of G-CSF in certain conditions increases the risk of myelodysplastic syndrome (MDS) and/or acute myeloid leukemia (AML). Hematopoietic progenitors from G-CSF-treated mice show evidence of DNA damage, which was demonstrated by increased double-strand breaks and recurrent chromosomal deletions. Concurrent treatment with genistein limits DNA damage in this population [96].

Quercetin

Quercetin (QC), a plant-derived bioflavonoid, is known for its ROS scavenging properties and has various antitumor properties in different solid tumors. The large amounts of ROS make cancer cells extremely susceptible to quercetin, one of the most available dietary flavonoids [97]. Quercetin could reverse docetaxel resistance in prostate cancer in proliferation, colony formation, migration, invasion, and apoptosis [98]. Targeting breast cancer stem cells with the CD44+/CD24- phenotype is critical for completely eradicating cancer cells due to their self-renewal, differentiation, and therapeutic resistance ability. Adding Quercetin to Doxorubicin is a practical approach for treating CSCs and bulk tumor cells [99].

Ginger (6-Gingerol)

6-Gingerol is the major pharmacologically active component of ginger (Zingiber officinale). Cisplatin and 6-gingerol combination is more effective in inducing apoptosis and suppressing the angiogenesis of ovarian cancer cells than using each drug alone [100]. The cytotoxic effects of 6-gingerol on Breast CSCs (BCSCs) from MCF-7 breast cancer cells and BCSCs showed selective killing of BCSCs that expressed the surface antigen CD44(+)/CD24(-), which is a marker combination for stem cells in general. 6-gingerol decreased the expression of the surface antigen CD44 on BCSCs and promoted β-catenin phosphorylation through the inhibition of hedgehog/Akt/GSK3β signaling, which are essential in cell proliferation during development but are activated during carcinogenesis. The inhibition decreases the cancer-related protein expression of downstream c-Myc (an oncogene) and cyclin D1(cell cycle activator protein) and reduces the native stem cell nature of BCSCs [101]. 6-Gingerol induced reactive oxygen species generation, the DNA damage response, cell cycle arrest, and the intrinsic pathway of apoptosis in embryonic CSCs. Furthermore, 6-gingerol inhibited iron metabolism and induced the Phosphatase and Tensin Homolog (PTEN), a vital tumor suppressor, which plays a crucial role in the induction of cell death [102].

Berberine

Berberine, an isoquinoline alkaloid present in various trees' stems, roots, and bark and extracted from the Chinese herbal medicine Coptis chinensis, was found to have antitumor activities against colorectal cancer [103]. Berberine could exert anticancer activities by regulating tumor cell proliferation, apoptosis, autophagy, metastasis, angiogenesis, and immune responses via modulating several signaling pathways within the tumor microenvironment [104]. Berberine suppresses cancer cell proliferation through inhibiting the synthesis of fatty acids and decreasing biogenesis and secretion of extracellular vesicles at 5-10 μmol/L, which exhibits a substantial anti-proliferative effect against the human colon cancer cell line HCT116 [105]. The use of berberine against neuroblastoma is through inhibition of fundamental characteristics of cancer stem cells, such as tumorigenicity, failure to differentiate, and reversal in the Epithelial- Mesenchymal Transition (EMT) with a decrease in tumor aggressiveness, metastasis, and resistance to therapy [106]. Berberine suppresses lipid metabolism by downregulating lipid uptake and alleviates the aging of adipose tissue and adipose-derived stem cells. These ultimately lead to the improvement of tumor-infiltrating immune cells, such as cytotoxic T-lymphocytes, to destroy advanced ovarian cancer in peritoneal metastasis and malignant ascites [107].

Sulforaphane

Sulforaphane is found in cruciferous vegetables like broccoli and Brussels sprouts. Sulforaphane is shown to inhibit the growth of cancer stem cells and induce apoptosis by activating detoxifying enzymes and modulating signaling pathways. It has been widely studied for its potential as a neuroprotective and anticancer agent [108]. Expression levels of gastric CSC markers significantly decreased after Sulforaphane treatment, which exerted inhibitory effects by suppressing proliferation and inducing apoptosis in gastric CSCs. It inhibited the activation of Sonic Hedgehog, a key signaling molecule in embryonic development, and maintained the stem cell nature of gastric CSCs [109].

Other CSCs inhibitors

We believe the main CSC inhibitors are presented above. Others include dietary constituents such as vitamins A and D, sulforaphane, piperine, Artemisinin, theanine, Thymoquinone (black seed oil), Lycopene (tomatoes and red fruits), Silymarin (milk thistle) and Choline have been shown to modify self-renewal properties of cancer stem cells and may be reviewed separately [110-115]. Asia is the most populous continent in the world, and some Asian countries do not have the resources to implement cancer screening programs for early detection or treatment. In addition, despite the excellent cancer preventive screening strategies in some Asian countries, well-designed clinical trials for cancer prevention are somewhat delayed compared to Western countries. Several neutraceuticals produced include Korean red ginseng, Curcumin, black or green tea (popular in Japan/Sri Lanka), Genistein from tofu (famous Chinese food), diallylsulfide or S-allylcysteine (garlic, popularly consumed as a food ingredient in many Asian countries), capsaicin, 6-gingerol, flavopiridol, and silymarin (abundant in various Asian foods). In Western countries, cancer chemotherapeutics involve strategies not only to block the growth of the primary tumor but also to inhibit its progression to metastatic disease. The endless pursuit of effective agents for cancer prevention may be a unique strategy in Asia. More active efforts for clinical application of

these principles should be supported [114, 115]. Hopefully, we will devote equal time to understanding why half of us never get cancer, while trying to stop cancer once it is detected. A better understanding of how we can use Natural Killer Cells (NKCs) and the rest of the immune system to prevent and fight cancer will be a significant component in conquering this dreaded disease. Our discovery of the NKC and developing nutraceuticals to boost NKC activity is synergestic with most nutraceuticals used to kill CSCs.

NKCs KILL CSCs

Natural Killer (NK) cells are a type of lymphocyte (a white blood cell) that play a crucial role in the innate immune response, particularly in recognizing and destroying infected or malignant cells. There is ongoing research into the ability of NKCs and CSCs to target and kill CSCs, a subpopulation of cancer cells believed to be responsible for tumor initiation, metastasis, and recurrence. NKC can recognize and destroy any cell type that exhibits non-self surface markers or stress-induced ligands, including some cancer cells and potentially CSCs. NKC can directly bind and destroy foreign cells, whether cancer cells or virus-infected cells, using cytotoxicity, apoptosis, and cytokine production to recruit other immune reactions against the foreign cell [33- 36].

Conclusions

Over 90% of pharmaceutical drugs are not water-soluble and require an oral dosage in most treatments. Over 60% of people struggle to swallow pills. This is especially true for older adults who may require over 20 pills per day. The consumption of such a large number of pills gives older adults the feeling of being "full," and nutritional wasting can occur. The pharmaceutical drug industry suffers from a lack of bioavailability, which requires higher dosages of a drug, with its inherent pitfalls of drugs being broken down in the stomach into potentially dangerous metabolites. One only has to watch the next television advertisement for a new drug to see this problem. The inability to minimize side effects makes FDA approval a lengthy process that can expose pharmaceutical companies to expensive class action lawsuits due to the irreparable harm experienced by patients. Drugs produced in pill form are difficult to modify the dosage without remanufacturing them. Biologic drugs require intravenous injections, which present issues related to proper bioavailability to the targeted cells.

The NutraNanoSphere (NNS) pharmacology will help address the above problems based on the features illustrated in Figure 15.

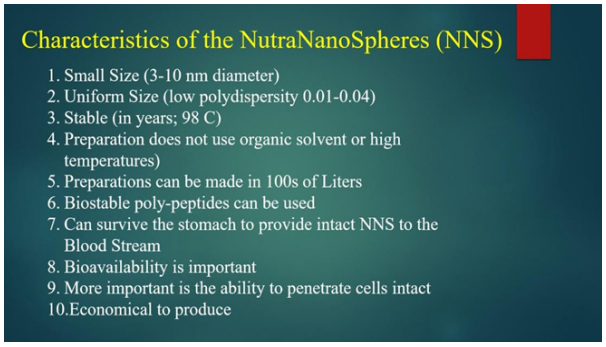

Figure 15: Characteristics of the NutraNanoSpheres™.

In Figure 15, the NNS can micellize various compounds in a proprietary produced sphere, which only requires a slightly elevated temperature and no organic solvents that may degrade the nutraceutical, peptide, or protein of interest. The result is the production of very stable NNS that can stay intact for years. Shipment can accomplished at room temperature or occasionally elevated temperatures. The NNS spheres are stable up to 98 °C and can be used for the online hot fill sterilization requirements [180-205 °F (82-95 °C) for 30 seconds] for nutritional drinks. We recommend shipping all our products at room temperature, accompanied by an indicator to show temperature exposure above 90°F (32°C). The NNS Products should be stored at 4 °C (do not freeze) and shipped at room temperature. If an NNS product is being used within 30 days, it can be stored at room temperature in the dark. An antibacterial agent, such as 0.1% sodium benzoate, works well with the NNS.

Most NNS are in the 3-10 nm diameter range, with larger diameters found when multiple NNS types are prepared, as in the case of the antimalarial TriAntiVP (28.1 nm). The NNS have low polydispersity (uniform size), usually ranging from 0.01 to around 0.20.

Figure 16 shows the difference between bioavailability and our new concept, accessibility. We have found that the NNS must function fully if it passes into the cell as an intact NNS. We are still discovering the reason for this, as seen by Curcumin and Vitamin C. Bioavailability is important, while Accessibility is much more important. NNS can penetrate all cells, whether normal or cancerous that can be many thousands. The contents and the NNS micelles can be a nutrient for normal cells, while being a poison for cancer or viral-infected cells. The NNS components also act to stimulate the production of normal stem cells, which will be presented in a future article.

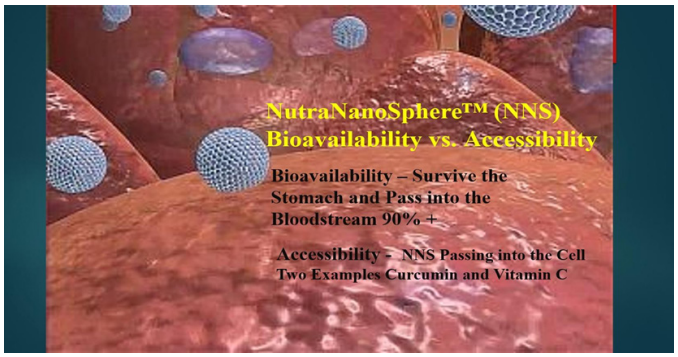

Figure 16: The NutraNanoSphere™ (NNS) has two primary functions: Bioavailability and Accessibility.

Acknowledgements

We thank Roberta Audate, Dr Wildert Charles, Dr. Valarie Chadic, and the Ministry of Health in Haiti, for treating babies, children, and adults for P. falciparum. We thank the Nigerian Ministry of Health, Professor Alebiosu, Chairman of the UNIOSUN HREC Committee, and the College of Health Sciences at the Osun State University in Osogbo, Nigeria. We thank Professor O.A. T. Alli and Dr. A. A. Ayankunle both of the College of Health sciences, Osun

State University, Osogbo. Nigeria. Special thanks to the Doctors, Nurses, and staff who successfully maintained compliance with the study protocol presented herein. Special thanks to Bonita, my wife of 55 years, my daughter, Andrea, and son, Kyle, with our grandsons Easton, Zeke, and Evan for their untiring support of my research. We thank Gary Chamblee for his support, Eddie Fuller at Brothers Printing for artwork, Nathan Clark for serving on our board and providing legal work, Harvey Birnholtz/ Mike Hewitt for their accounting assistance, and the IT guidance by Daniel Simons. We thank Dr. Larry Loomis, Dr. Tony Kirk, Bonita Thornthwaite, and Patty O'Neal for carefully proofreading this manuscript and laboratory contributions. We thank the Dolores Woolems family, The Shumard Foundation, Celia Lare, Jackie Rinck, and Dr. Bradford Weeks for their kind donations. We thank Todd Dossier, Joseph Harker, Dr. Brett Yunker of Strike Photonics, Carlton Morris, and Dr. John Kressler for continuing this research. This study is dedicated to the Memory of Roberta Audate.

References

1. Lipinski CA. Drug-like properties and the causes of poor solubility and poor permeability. Journal of Pharmacological and Toxicological Methods. 2000; 44: 235-249.
2. Stegemann S, Gosch M, Breitkreutz J. Swallowing dysfunction and dysphagia is an unrecognized challenge for oral drug therapy. Int J Pharm. 2012; 430: 197-206.
3. Schiele JT, Quinzler R, Klimm HD, et al. Difficulties swallowing solid oral dosage forms in a general practice population: prevalence, causes, and relationship to dosage forms. Eur J Clin Pharmacol. 2013; 69: 937-948.
4. Savjani KT, Gajjar AK, Savjani JK. Drug Solubility: Importance and Enhancement Techniques. ISRN Pharmaceutics. 2012; 1-10.
5. Lipinski CA. Drug-like properties and the causes of poor solubility and poor permeability. Journal of Pharmacological and Toxicological Methods. 2000; 44: 235-249.
6. https://www.fda.gov/consumers/consumer-updates/dont-be-alarmed-if-you-see-pill-your-stool
7. https://www.mayoclinic.org/diseases-conditions/constipation/expert-answers/pills-instool/faq-20057923
8. Dann O, Bergen G, Demant E, et al. Trypanocide diamidine dyes 2 phenylbenzofurans and 2 phenyl-indols. Justus Leibigs Ann Chem. 1971; 748: 68-79.
9. Thornthwaite JT, Sugarbaker EV, Temple WJ. Preparation of Tissues for DNA Flow Cytometric Analysis. Cytometry. 1980; 1: 229-237.
10. Thornthwaite JT, Thomas RA. High-Resolution DNA Measurements Using the Nuclear Isolation Medium, DAPI, with the RATCOM Flow Cytometer. Methods Cell Biol. 1990; 33: 111-119.
11. Thornthwaite JT, Russo J, Thomasal RA. A Review of DNA Flow Cytometric Preparatory and Analytical Methods. Immuno-cytochemistry in Tumor Diagnosis. 1985; 34: 380-398.
12. Hollenbeck CB. An introduction to the nutrition and metabolism of Choline. Cent Nerv Syst Agents Med Chem. 2012; 12: 100-113.
13. Nanavare P, Choudhury AR, Sarkar S, et al. Structure and Orientation of Water and Choline Chloride Molecules around a Methane Hydrophobe: A Computer Simulation Study. Chemphyschem. 2022; 23: 202200446.
14. Felipe A, Lovenduski CA, Baker JL, et al. Long-ranged heterogeneous structure in aqueous solutions of the deep eutectic solvent choline and geranate at the liquid-vapor interface. Phys Chem Chem Phys. 2022; 24: 13720-13729.
15. Chen J, Zeng X, Chen L. Evolution of microstructures and hydrogen bond interactions within choline amino acid ionic liquid and water mixtures. Phys Chem Chem Phys. 2022; 24: 17792-17808.
16. Bernhard W, Raith M, Shunova A, et al. Choline Kinetics in Neonatal Liver, Brain and Lung-Lessons from a Rodent Model for Neonatal Care. Nutrients. 2022; 14: 720.
17. Black SA, Rylett RJ. Choline transporter CHT regulation and function in cholinergic neurons. Cent Nerv Syst Agents Med Chem. 2012; 12: 114-121.
18. Imbard A, Benoist JF, Blom HJ. Neural tube defects, folic acid and methylation. Int J Environ Res Public Health. 2013; 10: 4352-4389.
19. Bekdash RA. Neuroprotective Effects of Choline and Other Methyl Donors. Nutrients. 2019; 11: 2995.
20. Imbard A, Benoist JF, Blom HJ. Neural tube defects, folic acid and methylation. Int J Environ Res Public Health. 2013; 10: 4352-4389.
21. Ridgway ND. The role of phosphatidylcholine and choline metabolites to cell proliferation and survival. Crit Rev Biochem Mol Biol. 2013; 48: 20-38.
22. Bernhard W, Poets CF, Franz AR. Choline and choline-related nutrients in regular and preterm infant growth. Eur J Nutr. 2019; 58: 931-945.
23. Peterson M, Warf BC, Schiff SJ. Normative human brain volume growth. J Neurosurg Pediatr. 2018; 21: 478-485.
24. Derbyshire E, Obeid R. Choline, Neurological Development and Brain Function: A Systematic Review Focusing on the First 1000 Days. Nutrients. 2020; 12: 1731.
25. Conlay LA, Sabounjian LA, Wurtman RJ. Exercise and neuromodulators: Choline and acetylcholine in marathon runners. Int J Sports Med. 1992; 1: 141-142.
26. Szyszka Ł, Górecki M, Cmoch P, et al. Fluorescent Molecular Cages with Sucrose and Cyclotriveratrylene Units for the Selective Recognition of Choline and Acetylcholine. J Org Chem. 2021; 86: 5129-5141.
27. Olufemi EO, Thornthwaite JT, Ayankunle OATA. Antimalarial Treatment in SouthWestern Nigeria. Microbiol Infect Dis. 2019; 3: 1-7.
28. Chadic V, Thornthwaite JT. ODSAC Document Summary showing 120 patients including children and adults cured of malaria. 2020.
29. Jerry T Thornthwaite, Daniel Strasser, Larry Loomis. How to Kill A Virus: Strengthening the Immune System, Reducing Inflammation, Relieving Oxidative Stress, Early Detection

and Treatment of SARS-CoV-2 (COVID-19). Acta Scientific Microbiology. 2021; 6-18.

30. Jerry T Thornthwaite, Daniel Strasser. Herpes/SARS-CoV-2 Treatment with Micellized Nutraceuticals. Acta Sci Micro. 2022; 5: 55-63.
31. Thornthwaite JT, Olufemi EO, Ayankunle AA, et al. DNA Gene Expression to Study Immunologic Mechanisms for the Long-term Cure of Malaria in Babies and Children in South-Western Nigeria. Adv Biol Chemistry. 2019; 9: 1-20.
32. Sugarbaker EV, Thornthwaite JT, Ketcham AS. Transient Changes in Tumor-Cell Characteristics During Spontaneous Pulmonary Metastasis Formation. Surgical Forum. 1979; 30: 134-136.
33. Thornthwaite JT, Leif RC. Characterization of Immune Cells Using the Plaque Cytogram Assay. Reticulendothelial Society. 1972.
34. Thornthwaite JT, Leif RC. The Plaque Cytogram Assay I. Light and Scanning Electron Microscopy of Immunocompetent Cells. J Immunol. 1974; 113: 1897-1907.
35. Thornthwaite JT, Leif, RC. Plaque Cytogram Assay II. Correlation Between Morphology and Density of Antibody-producing Cells. J Immunol. 1975; 114: 1023-1033.
36. Thornthwaite JT, Shah H, Shah P, et al. The Natural KillerCell: A Historical Perspective and the Use of Supplements to Enhance NKC Activity. Journal of Immune Based Therapies, Vaccines and Antimicrobials. 2012; 1: 21-52.
37. Thornthwaite JT, Shah H, England S, et al. Anticancer Effects of the Curcumin, Artemisinin, Genistein, and Resveratrol, and Vitamin C: Free vs. Liposomal Forms. Adv Biol Chemistry. 2017; 7: 27-41.
38. Ros M, Riesco Llach G, Polonio Alcalá E, et al. Inhibition of Cancer Stem-like Cells by Curcumin and Other Polyphenol Derivatives in MDA-MB-231 TNBC Cells. Int J Mol Sci. 2024; 25: 7446.
39. Ravindran J, Prasad S, Aggarwal BB. Curcumin and cancer cells: how many ways can curry kill tumor cells selectively?. AAPS J. 2009; 11: 495-510.
40. Mao X, Zhang X, Zheng X, et al. Curcumin suppresses LGR5(+) colorectal cancer stem cells by inducing autophagy and via repressing TFAP2A-mediated ECM pathway. J Nat Med. 2021; 75: 590-601.
41. Li Y, Wicha MS, Schwartz SJ, et al. Implications of cancer stem cell theory for cancer chemoprevention by natural dietary compounds. J Nutr Biochem. 2011; 22: 799-806.
42. Giordano A, Tommonaro G. Curcumin and Cancer. Nutrients. 2019; 11: 2376.
43. Mortezaee K, Salehi E, Mirtavoos Mahyari H, et al. Mechanisms of apoptosis modulation by Curcumin: Implications for cancer therapy. J Cell Physiol. 2019; 234: 12537-12550.
44. Wang S, Wu W, Liu Y, et al. Curcumin Induces Apoptosis by Suppressing XRCC4 Expression in Hepatocellular Carcinoma. Nutr Cancer. 2023; 75: 1958- 1967.
45. Haghighian HK, Ketabchi N, Kavianpour M. The Role of the Curcumin for Inducing Apoptosis in Acute Lymphoblastic Leukemia Cells: A Systematic Review. Nutr Cancer. 2021; 73: 1081-1091.
46. Li M, Guo T, Lin J, et al. Curcumin inhibits the invasion and metastasis of triple negative breast cancer via Hedgehog/Gli1 signaling pathway. J Ethnopharmacol. 2022; 283: 114689.
47. Zhang C, Hao Y, Wu L, et al. Curcumin induces apoptosis and inhibits angiogenesis in murine malignant mesothelioma. Int J Oncol. 2018; 53: 2531-2541.
48. Farghadani R, Naidu R. Curcumin as an Enhancer of Therapeutic Efficiency of Chemotherapy Drugs in Breast Cancer. Int J Mol Sci. 2022; 23: 2144.
49. Kong WY, Ngai SC, Goh BH, et al. Is Curcumin the Answer to Future Chemotherapy Cocktail?. Molecules. 2021; 26: 4329.
50. Zheng X, Yang X, Lin J, et al. Low curcumin concentration enhances the anticancer effect of 5-fluorouracil against colorectal cancer. Phytomedicine. 2021; 85: 153547.
51. Yan Z, Xiao P, Ji P, et al. Enhanced breast cancer therapy using multifunctional lipid-coated nanoparticles combining curcumin chemotherapy and nitric oxide gas delivery. Sci Rep. 2024; 14: 18107.
52. Peng Y, Ao M, Dong B, et al. Anti-Inflammatory Effects of Curcumin in the Inflammatory Diseases: Status, Limitations and Countermeasures. Drug Des Devel Ther. 2021; 15: 4503-4525.
53. Dehzad MJ, Ghalandari H, Nouri M, et al. Antioxidant and anti-inflammatory effects of curcumin/turmeric supplementation in adults: A GRADE-assessed systematic review 35 and dose-response meta-analysis of randomized controlled trials. Cytokine. 2023; 164: 156144.
54. Sadeghi M, Dehnavi S, Asadirad A, et al. Curcumin and chemokines: mechanism of action and therapeutic potential in inflammatory diseases. Inflammopharmacology. 2023; 31: 1069-1093.
55. Panknin TM, Howe CL, Hauer M, et al. Curcumin Supplementation and Human Disease: A Scoping Review of Clinical Trials. Int J Mol Sci. 2023; 24: 4476.
56. Jagetia GC. Radioprotection and radiosensitization by Curcumin. Adv Exp Med Biol. 2007; 595: 301-320.
57. Liu X, Cui H, Li M, et al. Tumor killing by a dietary curcumin mono-carbonyl analog that works as a selective ROS generator via TrxR inhibition. Eur J Med Chem. 2023; 250: 115191.
58. Liu X, Cui H, Li M, et al. Tumor killing by a dietary curcumin mono-carbonyl analog that works as a selective ROS generator via TrxR inhibition. Eur J Med Chem. 2023; 250: 115191.
59. Mukherjee S, Baidoo J, Fried A, et al. Curcumin changes the polarity of tumor-associated microglia and eliminates glioblastoma. Int J Cancer. 2016; 139: 2838-2849.
60. Zheng Y, Williams GR, Hu R, et al. Acid-Unlocked Two-Layer Ca-Loaded Nanoplatform to Interfere With Mitochondria for Synergistic Tumor Therapy. Int J Nanomedicine. 2025; 20: 1899-1920.

61. Giordano A, Tommonaro G. Curcumin and Cancer. Nutrients. 2019; 11: 2376.
62. Patel SS, Acharya A, Ray RS, et al. Cellular and molecular mechanisms of Curcumin in prevention and treatment of disease. Crit Rev Food Sci Nutr. 2020; 60: 887-939.
63. Fatima F, Chourasiya NK, Mishra M, et al. Curcumin and its Derivatives Targeting Multiple Signaling Pathways to Elicit Anticancer 36 Activity: A Comprehensive Perspective. Curr Med Chem. 2024; 31: 3668-3714.
64. Wang M, Jiang S, Zhou L, et al. Potential Mechanisms of Action of Curcumin for Cancer Prevention: Focus on Cellular Signaling Pathways and miRNAs. Int J Biol Sci. 2019; 15: 1200-1214.
65. Heng MC. Curcumin targeted signaling pathways: basis for anti-photoaging and anticarcinogenic therapy. Int J Dermatol. 2010; 49: 608-622.
66. Ming T, Tao Q, Tang S, et al. Curcumin: An epigenetic regulator and its application in cancer. Biomed Pharmacother. 2022; 156: 113956.
67. Li J, Chai R, Chen Y, Zhao S, Bian Y, Wang X. Curcumin Targeting Non-Coding RNAs in Colorectal Cancer: Therapeutic and Biomarker Implications. Biomolecules. 2022; 12: 1339.
68. Zhang W, Cui N, Ye J, et al. Curcumin's prevention of inflammationdriven early gastric cancer and its molecular mechanism. Chin Herb Med. 2022; 14: 244-253.
69. Passos CLA, Polinati RM, Ferreira C, et al. Curcumin and melphalan cotreatment induces cell cycle arrest and apoptosis in MDA-MB-231 breast cancer cells. Sci Rep. 2023; 13: 13446.
70. Zhang Q, Hui M, Chen G, et al. Curcumin-Piperlongumine Hybrid Molecule Increases Cell Cycle Arrest and Apoptosis in Lung Cancer through JNK/c-Jun Signaling Pathway. J Agric Food Chem. 2024; 72: 7244-7255.
71. Chandramohan S, Chatterjee O, Pajaniradje S, et al. Role of indole curcumin in the epigenetic activation of apoptosis and cell cycle regulating genes. J Cancer Res Ther. 2023; 19: 601-609.
72. Yazdani Y, Zamani ARN, Majidi Z, et al. Curcumin and targeting of molecular and metabolic pathways in multiple sclerosis. Cell Biochem Funct. 2023; 41: 779-787.
73. Vera Ramirez L, Pérez Lopez P, Varela Lopez A, et al. Curcumin and liver disease. Biofactors. 2013; 39: 88-100.
74. Lelli D, Pedone C, Sahebkar A. Curcumin and treatment of melanoma: The potential role of microRNAs. Biomed Pharmacother. 2017; 88: 832-834.
75. Kumar A, Harsha C, Parama D, et al. Current clinical developments in curcumin-based therapeutics for cancer and chronic diseases. Phytother Res. 2021; 35: 6768-6801.
76. Kumar A, Hegde M, Parama D, et al. Curcumin: The Golden Nutraceutical on the Road to Cancer Prevention and Therapeutics. A Clinical Perspective. Crit Rev Oncog. 2022; 27: 33-63.
77. Lee Y. Role of Vitamin C in Targeting Cancer Stem Cells and Cellular Plasticity. Cancers (Basel). 2023; 15: 5657.
78. Kaźmierczak Barańska J, Boguszewska K, Adamus Grabicka A, et al. Two Faces of Vitamin C—Antioxidative and Pro-Oxidative Agent. Nutrients. 2020; 12: 1501.
79. Chen Q, Espey MG, Sun AY, et al. Pharmacologic doses of ascorbate act as a prooxidant and decrease growth of aggressive tumor xenografts in mice. Proc. Natl Acad Sci USA. 2008; 105: 11105-11109.
80. Cazzato G, Lettini T, Colagrande A, et al. Immunohistochemical Expression of Programmed Cell Death Ligand 1 (PD-L1) in Human Cutaneous Malignant Melanoma: A Narrative Review with Historical Perspectives. Genes (Basel). 2023; 14: 1252.
81. Fu J, Wu Z, Liu J, et al. Vitamin C: A stem cell promoter in cancer metastasis and immunotherapy. Biomed Pharmacother. 2020; 131: 110588.
82. Gao Y, Yang L, Chen L, et al. Vitamin C facilitates pluripotent stem cell maintenance by promoting pluripotency gene transcription. Biochimie, 95 (11) (2013), pp. 2107-2113
83. Bhaskara VK, Mittal B, Mysorekar VV, et al. Resveratrol, cancer and cancer stem cells: A review on past to future. Curr Res Food Sci. 2020; 3: 284-295.
84. Rezakhani L, Salmani S, Eliyasi Dashtaki M, et al. Resveratrol: Targeting Cancer Stem Cells and ncRNAs to Overcome Cancer Drug Resistance. Curr Mol Med. 2024; 24: 951-961.
85. Xie C, Liang C, Wang R, et al. Resveratrol suppresses lung cancer by targeting cancer stem-like cells and regulating tumor microenvironment. J Nutr Biochem. 2023; 112: 109211.
86. Xie C, Liang C, Wang R, et al. Resveratrol suppresses lung cancer by targeting cancer stem-like cells and regulating tumor microenvironment. J Nutr Biochem. 2023; 112: 109211.
87. Naujokat C, McKee DL. The "Big Five" Phytochemicals Targeting Cancer Stem Cells: Curcumin, EGCG, Sulforaphane, Resveratrol and Genistein. Curr Med Chem. 2021; 28: 4321-4342.
88. Gan RY, Li HB, Sui ZQ, et al. Absorption, metabolism, anticancer effect and molecular targets of epigallocatechin gallate (EGCG): An updated review. Crit Rev Food Sci Nutr. 2018; 58: 924-941.
89. Fujiki H, Watanabe T, Sueoka E, et al. Cancer Prevention with Green Tea and Its Principal Constituent, EGCG: from Early Investigations to Current Focus on Human Cancer Stem Cells. Mol Cells. 2018; 41: 73-82.
90. Gu HF, Mao XY, Du M. Prevention of breast cancer by dietary polyphenols-role of cancer stem cells. Crit Rev Food Sci Nutr. 2020; 60: 810-825.
91. Toden S, Tran HM, Tovar Camargo OA, et al. Epigallocatechin-3-gallate targets cancer stem-like cells and enhances 5-fluorouracil chemosensitivity in colorectal cancer. Oncotarget. 2016; 7: 16158-16171.
92. Kumazoe M, Takai M, Hiroi S, et al. PDE3 inhibitor and EGCG combination treatment suppress cancer stem cell properties in pancreatic ductal adenocarcinoma. Sci Rep. 2017; 7: 1917.

93. Zhang Q, Cao WS, Wang XQ, et al. Genistein inhibits nasopharyngeal cancer stem cells through sonic hedgehog signaling. Phytother Res. 2019; 33: 2783-2791.

94. Naponelli V, Piscazzi A, Mangieri D. Cellular and Molecular Mechanisms Modulated by Genistein in Cancer. Int J Mol Sci. 2025; 26: 1114.

95. Yu D, Shin HS, Lee YS, et al. Genistein attenuates cancer stem cell characteristics in gastric cancer through the downregulation of Gli1. Oncol Rep. 2014; 31: 673-678.

96. Souza LR, Silva E, Calloway E, et al. Genistein protects hematopoietic stem cells against G-CSF-induced DNA damage. Cancer Prev Res (Phila). 2014; 7: 534-544.

97. Biswas P, Dey D, Biswas PK, et al. A Comprehensive Analysis and Anticancer Activities of Quercetin in ROS-Mediated Cancer and Cancer Stem Cells. Int J Mol Sci. 2022; 23: 11746.

98. Lu X, Yang F, Chen D, et al. Quercetin reverses docetaxel resistance in prostate cancer via androgen receptor and PI3K/Akt signaling pathways. Int J Biol Sci. 2020; 16: 1121-1134.

99. Azizi E, Fouladdel S, Komeili Movahhed T, et al. Quercetin Effects on Cell Cycle Arrest and Apoptosis and Doxorubicin Activity in T47D Cancer Stem Cells. Asian Pac J Cancer Prev. 2022; 23: 4145-4154.

100. Salari Z, Khosravi A, Pourkhandani E, et al. The inhibitory effect of 6-gingerol and cisplatin on ovarian cancer and antitumor activity: In silico, in vitro, and in vivo. Front Oncol. 2023; 13: 1098429.

101. Wu CH, Hong BH, Ho CT, et al. Targeting cancer stem cells in breast cancer: potential anticancer properties of 6-shogaol and pterostilbene. J Agric Food Chem. 2015; 63: 2432-2441.

102. Sp N, Kang DY, Jo ES, et al. Pivotal Role of Iron Homeostasis in the Induction of Mitochondrial Apoptosis by 6-Gingerol Through PTEN Regulated PD-L1 Expression in Embryonic Cancer Cells. Front Oncol. 2021; 11: 781720. Ref for Berberine.

103. Zhao Z, Zeng J, Guo Q, et al. Berberine Suppresses Stemness and Tumorigenicity of Colorectal Cancer Stem-Like Cells by Inhibiting m6A Methylation. Front Oncol. 2021; 11: 775418.

104. Hsu CY, Pallathadka H, Gupta J, et al. Berberine and berberine nanoformulations in cancer therapy: Focusing on lung cancer. Phytother Res. 2024; 38: 4336-4350.

105. Gu S, Song X, Xie R, et al. Berberine inhibits cancer cells growth by suppressing fatty acid synthesis and biogenesis of extracellular vesicles. Life Sci. 2020; 257: 118122.

106. Naveen CR, Gaikwad S, Agrawal Rajput R. Berberine induces neuronal differentiation through inhibition of cancer stemness and epithelial-mesenchymal transition in neuroblastoma cells. Phytomedicine. 2016; 23: 736-744.

107. Zhang X, Xiong B, Cheng Y, et al. Berberine inhibits metastasis of ovarian cancer by blocking lipid metabolism, alleviating aging of adipose tissue and increasing tumor infiltrating immune cells. Transl Oncol. 2025; 56: 102380.

108. Otoo RA, Allen AR. Sulforaphane's Multifaceted Potential: From Neuroprotection to Anticancer Action. Molecules. 2023; 28: 6902.

109. Ge M, Zhang L, Cao L, et al. Sulforaphane inhibits gastric cancer stem cells via suppressing sonic hedgehog pathway. Int J Food Sci Nutr. 2019; 70: 570-578.

110. Chan MM, Chen R, Fong D. Targeting cancer stem cells with dietary phytochemical - Repositioned drug combinations. Cancer Lett. 2018; 433: 53-64.

111. Kumar G, Farooqui M, Rao CV. Role of Dietary Cancer-Preventive Phytochemicals in Pancreatic Cancer Stem Cells. Curr Pharmacol Rep. 2018; 4: 326-335.

112. Kim YS, Farrar W, Colburn NH, et al. Cancer stem cells: potential target for bioactive food components. J Nutr Biochem. 2012; 23: 691-698.

113. Dandawate PR, Subramaniam D, Jensen RA, et al. Targeting cancer stem cells and signaling pathways by phytochemicals: Novel approach for breast cancer therapy. Semin Cancer Biol. 2016; 41: 192-208.

114. Park JM, Lee HJ, Yoo JH, et al. Overview of gastrointestinal cancer prevention in Asia. Best Pract Res Clin Gastroenterol. 2015; 29: 855-867.

115. Xu C, Zhang H, Mu L, et al. Artemisinins as Anticancer Drugs: Novel Therapeutic Approaches, Molecular Mechanisms, and Clinical Trials. Front Pharmacol. 2020; 11: 529881.